Ocean acidification impacts sperm swimming performance and pH_i in the New Zealand sea urchin *Evechinus chloroticus*

Michael E. Hudson[1,2], Mary A. Sewell[1,*]

[1]School of Biological Sciences, University of Auckland, Private Bag 92019, Auckland, New Zealand

[2]Institute of Marine Science, University of Auckland, Private Bag 92019, Auckland, New Zealand

[*]Corresponding Author: Mary A. Sewell m.sewell@auckland.ac.nz

Summary statement

Sea urchin sperm performance and pH_i is reduced in ocean acidification conditions, with a high degree of individual variation in both measures. [22 words]

ORCID ID Numbers:

Mary A. Sewell https://orcid.org/0000-0002-1595-7951

Abstract

In sea urchins, spermatozoa are stored in the gonads in hypercapnic conditions (pH<7.0). During spawning, sperm are diluted in seawater of pH>8.0, and there is an alkalinization of the sperm's internal pH (pH_i) through the release of CO_2 and H^+. Previous research has shown that when pH_i is above 7.2-7.3, the dynein ATPase flagellar motors are activated, and the sperm become motile. It has been hypothesised that ocean acidification (OA), which decreases the pH of seawater, may have a narcotic effect on sea urchin sperm by impairing the ability to regulate pH_i, resulting in decreased motility and swimming speed. Here we use data collected from the same individuals to test the relationship between pH_i and sperm motility/performance in the New Zealand sea urchin *Evechinus chloroticus* (Valenciennes) under near- (2100) and far-future (2150) atmospheric pCO_2 conditions (RCP 8.5: pH 7.77, 7.51). Decreasing seawater pH significantly negatively impacted the proportion of motile sperm), and four of the six computer-assisted sperm analysis (CASA) sperm performance measures. In control conditions, sperm had an activated pH_i of 7.52. *E. chloroticus* sperm

could not defend pH_i in future OA conditions; there was a stepped decrease in the pH_i at pH 7.77, with no significant difference in mean pH_i between pH 7.77 and 7.51. Paired measurements in the same males showed a positive relationship between pH_i and sperm motility, but with a significant difference in the response between males. Differences in motility and sperm performance in OA conditions may impact fertilization success in a future ocean.

Introduction

Reproduction is a central part of a species' life cycle, with an egg being fertilized by a single sperm to produce a viable zygote. In most broadcast spawning and sperm-casting marine invertebrates, external fertilization depends on the flow environment into which the gametes are spawned and, at smaller spatial scales, biological traits such as sperm motility and chemotaxis to bring the gametes together (Bishop, 1998; Crimaldi and Zimmer, 2014). The process of spawning also shifts the sperm and eggs from the intracellular chemical environment of the adult reproductive organs into that of the surrounding seawater (Bishop, 1998; Crimaldi and Zimmer, 2014; Hurd et al., 2020).

Sea urchins have been used as a model system to study fertilization and early development in marine invertebrates since the mid-19th century (Monroy, 1986; Adams et al., 2019). Male and female sea urchins have an annual reproductive cycle, generally with mature gonads in the perivisceral coelom during the summer months (Chia and Bickell, 1983; Adams et al., 2019). In the male gonad, cellular respiration of the concentrated sperm is regulated through CO_2 tension; with high CO_2 (hypercapnia) and a low internal pH (pH_i) of <7.0 maintaining the sperm in a non-motile quiescent state (Chia and Bickell, 1983; Mohri and Yasumasu, 1963; Mita and Nakamura, 2001; Hurd et al., 2020).

Upon release to the surrounding seawater, the sperm cells experience a drastic environmental change: from K^+- rich (>30 mM), low- oxygen tension, and acidic conditions in the testes to the lower K^+ concentrations, oxygen- rich and basic pH of around 8.2 in seawater (Christen et al., 1982; Johnson et al., 1983; Tosti, 1994, Bögner, 2016). Spawning and the subsequent dilution of sperm in seawater results in the alkalinization of pH_i through the release of CO_2 and H^+ (Johnson et al., 1983; Trimmer and Vacquier, 1986). When pH_i is above 7.2-7.3, the dynein ATPase flagellar motors that produce swimming are activated, with the maximum rate of increase in motility and respiration at about pH 7.5 (Gibbons and Fronk, 1972; Christen et al., 1982, 1986; Neill and Vacquier, 2004; Nishigaki et al., 2014).

Because sperm are unicellular, they have a limited capacity to tolerate changes in pCO_2 and pH due to anthropogenic climate change (Melzner et al., 2009). In addition, hypercapnia, which has a narcotic effect within the gonad, may also impact sea urchin sperm released into ocean acidification (OA) conditions (increased pCO_2, decreased pH, Havenhand et al., 2008; Morita et al., 2010) through the failure to obtain the pH_i required for the activation of sperm swimming. The impaired ability to regulate pH_i may then have a narcotic effect on sea urchin sperm, resulting in decreased motility and swimming speed (Kurihara, 2008; Byrne, 2011; Reuter et al., 2011; Bögner, 2016; Hurd et al., 2020).

Here we test the relationship between pH_i and sperm motility in the New Zealand sea urchin *Evechinus chloroticus* (Valenciennes) under near- (2100) and far-future (2150) atmospheric pCO_2 conditions under Representative Concentration Pathway (RCP) 8.5 (IPCC 2014). We first developed a new methodology for measuring pH_i in sea urchin sperm using a fluorescent dye SNARF-1 (5-(and-6)-carboxy SNARF®-1) and a nigericin calibration which required concurrent development of an appropriate ionic buffer. Then, as there is increasing recognition of the importance of individual responses to climate change (e.g., Pistevos et al. 2011; Schlegel et al. 2012; Guscelli et al. 2019), we measured pH_i and performance in sperm from the same male [using SNARF-1 and computer-assisted sperm analysis (CASA, Partyka et al., 2012) respectively]. Sperm was activated by dilution in control and lower pH seawater (OA treatment) to test if there was a narcotic effect on sperm performance (e.g., decreased motility and swimming speed, Kurihara, 2008; Byrne, 2011; Reuter et al., 2011; Bögner, 2016; Hurd et al., 2020) due to the failure to achieve the pH_i required for activation of sperm swimming under OA conditions.

Methods

Seawater manipulation and chemistry

Protocols for manipulating and analyzing elevated pCO_2 experimental seawaters were based on recommendations from Dickson et al. (2007) and Riebesell et al. (2010). In brief, seawaters were bubbled with target CO_2 concentrations to produce three OA treatment seawaters: 1) Control = atmospheric CO_2 at time of experiments (2014, 380 µatm); 2) Business as usual emission scenario RCP 8.5 at 2100 (range 851 to 1370 µatm CO_2); 3) Business as usual emission scenario RCP 8.5 at 2150 (range 1371 to 2900 µatm CO_2; IPCC, 2014). Seawater for all experiments was obtained pre-filtered from Kelly Tarlton's Undersea World and re-filtered before pCO_2 manipulation through two nested, 1 µm filter bags (FSW).

Air was initially dried and stripped of CO_2 before being mixed with instrument grade CO_2 (99.98%) using a dial-a-gas mass flow controlled (Smart Trak2, Sierra Instruments, Monterey, CA, USA) mixing setup based on the experimental system outlined by Fangue et al. (2010) and calibrated with an infrared CO_2 analyser (Qubit S151, Qubit Systems Inc., Kingston, Ontario, Canada). To ensure the equilibrium of gas partial pressures between target gas mixtures and experimental seawaters, self-contained 20 L containers of FSW were bubbled for a minimum of 16 hours. Bubbling used a temperature-controlled (20 ± 1°C) circulation system where gas mixtures were added through a venturi injector (Mazzei, MK-384, Mazzei Injector Company, Bakersfield, CA, USA) to optimize gas exchange efficiency.

Sets of OA treatment waters (Control, RCP 8.5 at 2100 and RCP 8.5 at 2150) were handled as described in SOP1 (Dickson et al., 2007). OA seawaters were taken from the bubbling buckets with water samples siphoned through a silicone hose, over-filling 250 mL boro-silicate sample bottles by at least 50% for experiments and seawater analysis. A separate set of OA waters were prepared for each motility and pH_i experiment and were placed in a 20°C water bath (Grant W28, Grant Instruments (Cambridge) Ltd, Shepreth, UK) at least 2 h before experiments for temperature equalisation. Each set of bottles was held in a custom Styrofoam insulator to minimise temperature and CO_2 changes during the motility and pH_i experiments. Experimental aliquots were rapidly taken from the mid-water column for analysis. Water temperature (Thermapalm, Thermoworks, American Fork, UT; USA; certified calibrated accuracy 0.05 °C) and salinity (YSI 30, YSI Inc., Yellow Springs, OH, USA) were measured before experiments.

pH_{Total} and TA were determined from OA treatment waters for the calculation of seawater carbonate chemistry. All pH_{Total} analyses were performed within 2 h of sampling; TA samples (250 mL) were preserved with a 50 µL aliquot of saturated mercuric chloride and stored at 4 ˚C in the fridge for later analysis. Spectrophotometric pH_{Total} determination used *m*-cresol purple (Sigma) was based on SOP6b (Dickson et al., 2007) and Fangue et al. (2010); calibration was performed using TRIS standard (SOP3a) (Dickson et al., 2007) and accuracy confirmed against certified reference standards to be 8.104 pH (Dickson et al., 2007). Open-cell potentiometric TA measurements were run using a Mettler-Toledo T50 automated titrator (Mettler-Toledo International Inc., Columbus, OH, USA) based on SOP3b (Dickson et al., 2007) and Fangue et al. (2010) with the accuracy of TA values confirmed using Scripps certified reference seawater (batch 108 at TA = 2218 µmol/kg).

Carbonate chemistry for OA treatment waters was recalculated from measured parameters (salinity, temperature, pH_{Total}, TA) to experimental temperature points using the seacarb (v. 3.0.8) package in R (v. 3.1.2). The seacarb R package was selected based on comparisons of ten ocean carbonate chemistry packages by Orr et al. (2015) using CO_2 constants as outlined in "Guide for best practices for ocean CO_2 measurements" (Dickson et al., 2007). Seacarb uses the recommended formulations for first and second dissociation constants K_1 and K_2 (Lueker et al., 2000), K_f (Perez and Fraga, 1987), and K_s (Dickson, 1990). Additionally, the recommended (Dickson et al., 2007) boron/chlorinity ratio from Uppström (1974) and default values for atmospheric and hydrostatic pressures, silicate, and phosphorous content were used. All our experiments were within the specified salinity (19-43 ppt) and temperature (2-35 ˚C) limitations for constants K_1 and K_2 (Orr et al., 2015).

Sea urchin collection and spawning

During the austral summer of 2014-2015, adult *Evechinus chloroticus* were collected from the shallow subtidal (1-3 m depth) at Matheson's Bay (36°18'6.58" S; 174°48'0.71″ E) within the Hauraki Gulf, New Zealand. Seawater pH near the collection site on a representative day during the spawning season (28th November) averaged 8.040 ± 0.037 (SD; range 7.920-8.109; N= 1440) in the *Ecklonia* kelp forest, and 8.011 ± 0.046 (SD; range 7.822-8.081; N= 4320) at the seafloor (C. Blain, SeaFET data).

Adults were transported to the seawater facilities at the University of Auckland within 2 h of collection and maintained in aerated aquaria (80 L) in environmentally controlled conditions (18 °C, 12:12 dark:light cycle). Urchins were fed to satiation on seaweed (*Ecklonia radiata* and *Carpophyllum* spp.) and spawned using standard procedures (1-3 mL injection of 0.5 M KCl into coelom) within 2 weeks of collection. Sperm was collected dry from the aboral surface and stored in 1.5 mL Eppendorf tubes in an iced water bath.

Sample preparation

Paired sperm motility and pH_i measurements were made on thirteen different males during a 2-week period, as shown in Figure 1. Sperm quality was visually assessed for high levels of motility using a Sedgewick Rafter slide at 100 x magnification. Sperm concentration for all experiments was standardised through haemocytometer counts from a standard dilution of 10 µL dry sperm mixed with 30 mL FSW. From these counts, the volume of dry sperm to give a target sperm concentration of 1 million cells/ mL for

experiments was calculated for each male. Multiple males were run on a single day, with the order of OA seawaters randomly selected for each male. This order was repeated for the paired motility, pH_i measurements, nigericin calibration, and incubation controls for that male (Fig. 1).

Sperm motility and performance

Optimised video capture for sperm motility analysis used an inverted microscope (Nikon Eclipse T*i* at 5x magnification) adjusted for differential interference contrast (DIC) imagery, following the recommendations of Boryshpolets et al. (2013) and Castellini et al. (2011) for consistent within-experiment equipment setup and video capture frame rate. Sperm movement was captured in a 250 image TIF-stack with an ANDOR iXon camera at room temperature (20^{o}C) using proprietary IQ2 software with 2x2 binning to give a capture rate of 34 frames per second. To minimize the boundary (or wall) effect from glass surfaces (Gee and Zimmer-Faust, 1997; Elgeti et al., 2010) and maximise thermal inertia, we designed a set of custom, deep, and relatively large-volume imaging chambers to the size of a standard microscope slide (25 mm x 75 mm). Constructed from 3 mm thick PVC plastic, there were two 12 mm diameter chambers per plate, with a glued coverslip on the base and a removable coverslip on top. The chamber volume was ca 339 µL.

Motility recordings were performed as rapidly as logistically possible, with all video recordings started ~10 seconds after initiating each sperm dilution. The pre-calculated volume of dry sperm was added to a 14 mL aliquot of OA seawater in a 15 mL Falcon tube and agitated gently for 4 seconds to make a relatively homogenous sperm suspension of ~1 million cells/ mL. To minimise air bubbles when the chamber was closed with the top coverslip, a 350 µL aliquot of the sperm suspension was gently added to over-fill the imaging chamber, and the top coverslip lowered in place to close. The chamber was immediately put on the inverted microscope stage with the focus pre-set for midway between the two coverslips, and the 250 image TIF-stack acquisition started. Sperm dilutions were mixed in rapid succession producing back-to-back recordings with technical replication of 10 at each CO_2 treatment (Control, RCP 8.5 at 2100, RCP 8.5 at 2150; Fig. 1). Preliminary analyses showed a high degree of technical replication was required to characterise variance within males.

Computer-assisted sperm analysis (CASA) was performed in ImageJ (v. 1.50a running on FIJI "Fiji Is Just ImageJ"; National Institutes of Health, Bethesda, MD, USA), which produces outputs similar to commercially available systems (Boryshpolets et al., 2013). A customised batch-processing macro (inspired by: Purchase and Earle, 2012) incorporating the CASA plugin (Wilson-Leedy and Ingermann, 2007) was used to analyse a two-second sub-stack (images 18 to 85) of the original TIF-stacks. The CASA plugin was parameterised to identify *E. chloroticus* sperm cells and define motion characteristics for motile and non-motile sperm (Supplementary Materials and Methods 1). For each sample, output data on sperm swimming performance included the proportion of motile sperm, and CASA parameters, as described in Table 1.

Internal pH (pHi)

Internal pH (pH_i) of sperm was measured using a single laser flow cytometer and the pH-sensitive dye carboxy-SNARF-1 [(seminaphthorhodafluor), acetoxymethyl ester, acetate; Invitrogen, Molecular Probes C1272, Lot # 1151593, Waltham, MA, USA)]. SNARF-1 is ideal for analysing pH_i as the pKa of ~7.5 (Thermofisher Catalog) is approximately the activation pH_i in sea urchin sperm (Christen et al., 1982, 1983; Johnson et al., 1983; Lee et al., 1983), and the dye can be used to measure pH changes between pH 7 and pH 8.

Calibration of SNARF-1 fluorescence measurements used the polyether antibiotic nigericin (Bond and Varley, 2005). Nigericin acts as an ionophore to equalise H^+ concentrations (Thomas et al., 1979; Hamidinia et al., 2004), allowing the construction of a calibration curve for SNARF-1 fluorescence using pH buffers across the expected pH_i range. However, nigericin also equalises other cations, including Na^+ and K^+ (Pressman, 1976; Riddell et al., 1988; Negulescu and Machen, 1990). Therefore, to limit any nigericin-induced shifts in SNARF-1 fluorescence, resulting in an over-estimation of pH_i (Negulescu and Machen, 1990), we needed to formulate a buffer appropriate for *E. chloroticus* sperm. Changes in $[Na^+]_i$ and $[Ca^{2+}]_i$ were minimized by replacing NaCl with choline chloride, as choline blocks nigericin-induced across-membrane movement of Na^+ and Ca^{2+} (García-Soto et al., 1987; Pressman, 1976; Riddell et al., 1988). Nigericin also induces equalisation of internal and external $[K^+]$; therefore, $[K^+]$ of the buffers must equal $[K^+]_i$ of activated sperm (Thomas et al., 1979; Babcock, 1983; Negulescu and Machen, 1990). A review of existing literature for experimentally determined or referenced values of $[K^+]_i$ indicated a wide range (120 to 480 mM for marine invertebrate tissues) and a lack of certainty for an appropriate

$[K^+]_i$ to use for sea urchin sperm (Supplementary Materials and Methods 2, Table S3). Multiple analytical techniques were used to measure $[K^+]_i$ in *E. chloroticus* sperm (Supplementary Materials and Methods 2), with calculations based on average sperm volume (1.29 fL, Hudson et al., 2015), average sperm counts, and average sample K^+ content.

Full details of the optimization of SNARF-1 incubations, flow cytometer settings, and appropriate buffers for determining pH_i in *E. chloroticus* sperm are provided in Supplementary Materials and Methods 2. In brief, to minimise activation and metabolism of sperm before experimental incubations, dry sperm were minimally diluted and kept on ice. Every second day, a new 1.25 mM SNARF-1 stock was prepared in anhydrous dimethyl sulfoxide (DMSO, Sigma-Aldrich, Merck KGaA, Darmstadt, Germany) and stored in the dark at -18 °C between use. A standard 4 µL aliquot of dry sperm was added to 75.4 µL of FSW and 0.64 µL of stock SNARF-1 to give a final dye concentration of 10 µM in a brown 1.5 mL Eppendorf tube. The 10 µM final concentration for SNARF-1 was based on experiments in *E. chloroticus* sperm (see Supplementary Materials and Methods 2) and recommendations for 1-10 µM concentrations by the dye manufacturer (Thermofisher). A parallel incubation with the SNARF-1 replaced with FSW was used as a control (Fig. 1). Incubations were mixed well by hand and left in ice water for 90 minutes in the dark.

After the 90-minute SNARF-1 incubation, a predetermined volume of sperm (calculated for each male from haemocytometer counts, n=2, Fig. 1) was diluted in 3 mL of OA treatment water to give a target sperm concentration of 1 million cells/ mL. Immediately after mixing, samples were analysed in a flow cytometer (BD Biosciences FACS Calibur, Becton, Dickinson and Company, Franklin Lakes, NJ, USA) with a 488 nm argon laser, optimised for *E. chloroticus* sperm cells with a combination of forward and side scatter (FSC and SSC, respectively; Supplementary Materials and Methods 2). Stained sperm were identified using the SNARF-1 emission from detectors FL2 and FL3 (585/42 nm and 670 nm long-pass, respectively) with voltages adjusted for autofluorescence and position on the axes. An event rate of 350 to 150 events per second resulted in a single consolidated population of sperm cells identifiable by FSC and SSC. Data from approximately 5000 events were collected for each sample. As with the analysis of sperm motility, consecutive replicate dilutions (n = 10) were mixed for each OA seawater from the SNARF incubation mix (Fig. 1) and run in immediate succession followed by controls for 1) seawater alone, 2) sperm without SNARF-1 and 3) sperm viability confirmed with 1 mM propidium iodide (PI).

Flow cytometer output files (*.fcs*) were processed in FlowJo (version 10.0.8) by gating the single population of sperm cells using FSC and SSC. The SNARF-1 stained cells of this gated population were isolated by setting additional active gates on both FL2 and FL3 histograms based on the unstained control. A small proportion (average for FL2 and FL3 for each sample < 5 %) of the samples were unstained and excluded from further analysis. The SNARF-1 fluorescence ratio (R) was calculated from FL3/FL2 using the mean fluorescence intensities of the gated populations (e.g., Bond and Varley, 2005). R was calculated for all males in both control and OA treatment waters, as well as the calibration solutions.

pH_i was quantified from the fluorescence ratio R by calibrating pH buffers across the expected pH_i range using the ionophore nigericin, as described above. The use of nigericin calibration is well established (e.g., Weider et al., 1993; Bond and Varley, 2005; Chavez et al., 2020) and preferred for flow cytometry; however, the calibration solution is critical for pH_i determination (Bond and Varley, 2005). Nigericin calibration in *E. chloroticus* sperm required a buffer $[K^+]$ of >450 mM (Supplementary Materials and Methods 2). A final buffer formulation with $[K^+]$ of 472.5 mM consisted of 22.5 mM HEPES-KOH, 450 mM KCl, and 120 mM CoCl (modified from Nakajima et al., 2005). The buffer series was prepared to target pH values (6.81, 7.00, 7.26, 7.51, 7.75, 8.00, and 8.11) with 472.5 mM KCl in 3 M HCl and 3.472 M CoCl to standardise the combined volume added to each buffer. Calibration buffers were stored in the fridge, and two hours before experiments were put in the same 20°C water bath as OA treatment waters. A calibration was performed for each male at the end of the pH_i experiment (Fig. 1). A global pH_i calibration curve for all individuals was calculated from the 3rd order polynomial regression using a linear model in the statistical software 'R'.

Statistical analyses

Statistical analyses were performed using the software RStudio (version 0.99.486) and 'R' (RCoreTeam, 2015), unless specified otherwise, with basic plotting done using the ggplot2 package. Data from seawater pH_{Total} and pH_i calibrations were separately analysed with a one-way ANOVA. Assumptions of normality were checked with Q-Q plots and Shapiro-Wilk, and heteroscedasticity with Levene's test. Post hoc test for comparisons between means used Tukey-Kramer's ($\alpha = 0.05$).

The effect of elevated CO_2 seawater on sperm motility and pH_i was calculated on non-standardised data using the logarithmic response ratio (LnRR = ln[$\bar{x}$ treatment/$\bar{x}$ control]; Nakagawa and Cuthill, 2007; Schlegel et al., 2012; Sewell et al., 2021). Technical replicates were averaged to the level of the individual male and LnRR calculated for all sperm performance measures (CASA outputs from Table 1, pH_i, SNARF-1 fluorescence ratio R). Each parameter's LnRR for all 13 males was then boot-strapped in the statistical software 'R' running *boot* package, and the resulting mean and 95% normal confidence intervals returned from 100,000 iterations. The confidence intervals provide a measure of the variance between individuals, and results are interpreted as significant where CIs do not overlap with zero (Schlegel et al., 2015).

For multivariate analysis, all data were standardised to a mean of zero and a variance of 1 to prevent distortion of the analysis from 3 orders of magnitude difference between values for different parameters of sperm performance (Quinn and Keough, 2002). To reduce multi-collinearity, the seven CASA parameters (Table 1) for each technical replicate (N=9-10), OA treatment (N=3), and male (N=13) were condensed into principal components (PC) using a principal component analysis (PRIMER v. 6, Plymouth Marine Laboratory). A Euclidean distance matrix was then calculated for each male/OA treatment based on the average of the technical replicates for PCs and the pH_i. An initial permutational multivariate analysis of variance (PERMANOVA) was performed with two factors (male, OA treatment) using 9999 permutations of residuals under a reduced model. A lack of replication at the lowest level (i.e., due to the averaging of technical replicates to a single value) resulted in the automatic exclusion of the highest level interaction term due to being confounded by the variance of the residuals (Anderson et al., 2008). Multivariate dispersion using PERMDISP tested for homogeneity in the cluster dispersion around the centroids for the three OA treatments. A final analysis used PERMANOVA with pairwise comparisons of the factor OA treatment.

Results

Seawater chemistry

There was a clear and consistent separation between control and OA treatments during the experiments (Table 2), with a significant difference in pH_{Total} (ANOVA: $F_{(2,9)}$ = 727.4, $p < 0.0001$). There was a ΔpH of -0.32 pH units between the Control and RCP 8.5 at 2100 and a ΔpH of -0.58 pH units between the Control and RCP 8.5 at 2150 (Table 2).

Seawater was undersaturated in aragonite only in the RCP 8.5 at 2150 treatment (Ω_{Ar} <1, Table 2).

Sperm motility and performance

E. chloroticus sperm in all OA treatments swam with a high degree of directionality with a lack of circular paths suggesting the edge effect on swimming behaviour was avoided. Boot-strap analysis of LnRR showed significant negative effects on sperm motility in both RCP 8.5 treatments (CI does not overlap with zero, Fig. 2). In control conditions, the proportion of sperm that were motile was 0.83 (grand mean for 13 males, Table 3). Sperm in RCP 8.5 at 2100 (pH 7.77) had a reduced proportion of motile sperm (0.74); a decrease in proportion motile of 0.09 from the control (Table 3). Sperm in RCP 8.5 at 2150 (pH 7.51) showed a further decrease in the proportion motile to 0.64 (Table 3); a decrease in proportion motile of 0.19 from the control (Table 3).

CASA measures of sperm swimming performance were also altered under OA conditions (Table 3). Some measures showed greater variability between males, as shown by the size of the 95% confidence intervals in the LnRR (Fig. 2). In general, sperm performance was significantly negatively impacted by elevated pCO_2 seawaters, except for the positive, but non-significant changes, in the velocity measures VCL and VAP (Fig. 2). The significantly lower LIN (pH 7.77 = -0.2, pH 7.51 = -0.26) and VSL (pH 7.77 = -21.16, pH 7.51 = -29.12 $\mu m.s^{-1}$) suggest that the actual path taken by sperm was significantly more curved, with an overall significant decrease in the distance covered from the starting point (PROG, Fig. 2, Table 3).

All sperm parameters with a significant OA impact showed a maximum negative effect size at RCP 8.5 at 2100 (pH 7.77, Fig. 2). No significant differences in sperm performance effect size were seen between the pH 7.77 and pH 7.51 OA treatments (Fig. 2).

pH_i

Procedural controls showed no contamination of the OA seawaters (no, or very low events of FSC and SSC recorded) and high levels of sperm cell viability for all trials (minimal PI signal indicating intact cellular membranes; Supplementary Materials and Methods 2). The SNARF-1 fluorescence ratio (R) calibration curve, used for calculation of pH_i, showed a consistent relationship between males, with highly significant differences between R values for each buffer (Fig. 3, ANOVA: $F_{(6,98)} = 656.8$, $p < 0.0001$).

Sperm in control conditions had a pH_i of 7.52 (Table 3); which was -0.57 units lower than the seawater in which they were activated (control seawater pH 8.09, Table 1). Sperm in RCP 8.5 at 2100 and RCP 8.5 at 2150 treatments showed a smaller difference in pH_i relative to the pH of the OA treatment waters in which they were activated. Sperm in RCP 8.5 at 2100 had a pH_i of 7.35 (Table 3), -0.42 pH units below the OA seawater treatment (pH 7.77, Table 1). Sperm in RCP 8.5 at 2150, similarly, had a pH_i of 7.31 (Table 3), -0.2 pH units below the OA seawater treatment (pH 7.51, Table 1).

Sperm pH_i was significantly impacted by OA treatment, with all sperm exhibiting a similar effect size (LnRR) with relatively slight among-male variation (narrow CIs, Fig. 2, Table 3). A negative effect size for pH_i was observed at RCP 8.5 at 2100 (pH 7.77, Fig. 2),. However, there was no significant difference in the effect size for pH_i between the pH 7.77 and pH 7.51 OA treatments (Fig. 2); the same pattern as seen in the sperm performance parameters described above.

Overall quality and performance characteristics

Principal components analysis (PCA) on the seven CASA output variables (Table 1) resulted in three PCs with eigenvalues > 1 that together explained more than 75 % of the variation. PC1 was primarily influenced by the directionality of sperm (VSL, LIN, and PROG), PC2 by the negative contribution of non-linear measurements (VCL and VAP), and PC3 by the head movement and actual path taken (WOB and VCL, respectively); sperm motility contributed almost evenly to PC1 and PC3 (Table 4). pH_i had an eigenvalue < 1 (0.958) and explained a smaller % of the variation (14.1%, Table 4).

A principal coordinates analysis (PCO) analysis was then conducted based on PC1-PC3 from the PCA (above) and the independent measurement of pH_i. Most of the variation in sperm performance between OA treatments could be explained by PCO1 (63.4 %) and PCO2 (21.3 %, Fig. 4). There were no significant differences between males (pseudo $F_{(12,24)}$ = 0.0031, p = 1). However, there were highly significant differences between the three OA treatments (PERMANOVA: pseudo $F_{(2,24)}$ = 15.329, p = 0.0001), but with homogeneous multivariate dispersion (PERMDISP: $F_{(2,36)}$ = 0.001647; p(perm) = 0.9843), suggesting that differences between OA treatments can be attributed to both sperm motility (PCs) and pH_i. Pairwise comparison showed differences in sperm performance in both RCP 8.5 OA treatments compared to control [RCP 8.5 at 2100: t = 4.046, p (perm) = 0.0001. RCP 8.5 at

2150: t = 5.246, p (perm) = 0.0001], but not between the RCP 8.5 OA treatments [t = 1.319, p (perm) = 0.1651].

Individual variation

There was a positive relationship between pH_i and the proportion of sperm attaining activation (proportion motile) in all males (Fig. 5). However, there were significant differences between males in the slope of this relationship (PERMANOVA: pseudo $F_{(12,24)}$ = 6.0362, p = 0.0001, Fig. 5), reflecting male-to-male variation in the response of sperm to OA treatment.

Discussion

Activation of sperm of *Evechinus chloroticus* in OA treated seawaters had significant negative impacts on sperm motility, four of the six CASA sperm performance measures (VSL, LIN, WOB, PROG), and pH_i. In control conditions, sperm had an activated pH_i of 7.52; however, sperm in both RCP 8.5 OA treatments could not attain a pH_i of this magnitude. Instead, there was a stepped decrease in pH_i from the Control at RCP 8.5 at 2100 (pH 7.77), with no significant difference in mean pH_i in the two OA treatments (RCP 8.5 at 2100 and 2150, pH 7.7. and 7.51, respectively). Using paired data collected from the same individuals, we found a positive relationship between pH_i and sperm motility in *E. chloroticus*, but with a significant difference in the response between males.

Sperm motility and performance

In OA conditions, there was an overall decreased motility and reduced swimming performance of *E. chloroticus* sperm, but no significant change in through-the-water speed (VCL). OA experiments in other sea urchin species have shown a variable response in VCL: an increase in *Paracentrotus lividus* (Ireland, Graham et al., 2015), *Psammechinus miliaris* (Caldwell et al., 2011), and *Lytechinus pictus* (Smith et al., 2019), a decrease in *Heliocidaris erythrogramma* (Smith et al., 2019) and *Paracentrotus lividus* (Italy, Munari et al., 2022), or no significant change here in *E. chloroticus*.

Sperm of *E. chloroticus* in OA conditions swam a more curved path, so the straight-line speed between two points was effectively slower (reflected in lower VSL and PROG). Lower directionality (PROG and VSL), combined with a lower proportion of motile sperm, is modeled to negatively impact fertilisation success (Vogel et al., 1982; Levitan et al., 1991;

Lewis et al., 2002). Specifically, a decrease in the proportion of motile sperm lowers the effective sperm concentration, and decreased swimming speed reduces the rate constant for sperm-egg collisions $\beta_{0,}$ which is estimated from sperm swimming velocity (υ) and the cross-sectional area of the egg σ_0 (Vogel et al., 1982).

In an OA context, the direct impacts of lower sperm motility and/or speed correspond with lower fertilisation rates in *Heliocidaris erythrogramma* (Havenhand et al., 2008; Smith et al., 2019), *Lytechinus pictus* (Smith et al., 2019), and *Paracentrotus lividus* (Graham et al., 2015; Munari et al., 2022), or indirectly through the effect of sperm concentration on fertilisation rates in *Mesocentrotus franciscanus* (Reuter et al., 2011), *Heliocidaris erythrogramma* (Schlegel et al., 2012), and *Sterechinus neumayeri* (Ho et al., 2013; Sewell et al., 2014). The changing parameters of sperm performance may well have further implications for sperm limitation, polyspermy, and the plasticity of egg size (Millar and Anderson, 2003; Luttikhuizen et al., 2011; Reuter et al., 2011; Okamoto, 2016). For example, the faster VCL observed for sperm of sea urchins under OA conditions (Graham et al., 2015; Caldwell et al., 2011; Smith et al., 2019) will be a disadvantage in conditions of sperm limitation, as sperm longevity will be limited by more rapid depletion of finite endogenous energy stores (Fitzpatrick et al., 2012).

Broadcast-spawning marine invertebrates in OA conditions will release both the egg and the sperm into a lower pH environment. OA can also impact unfertilized eggs, including changes in pH_i (Bögner et al., 2014) and a reduction in the size of the jelly coat that contains sperm attracting chemicals (Foo et al., 2018a,b). Theoretical and experimental studies in sea urchins have suggested that larger jelly coats are a greater target for sperm and have a higher fertilization success (Levitan and Irvine, 2001; Podolsky, 2002; Deaker et al., 2019). As the jelly coat is the source of the chemical attractants used in chemotaxis in sea urchins (Miller, 1985; Wood et al., 2015; Ramírez-Gómez et al., 2020), a reduction in the size of the jelly coat, in combination with decreased sperm performance (motility, speed), may have a major impact on fertilization success in OA conditions.

In these experiments we measured sperm motility after activation in control and OA seawaters. As noted above, chemotaxis of sperm towards eggs has been shown in a number of sea urchin species (Miller, 1985; Wood et al., 2015; Ramírez-Gómez et al., 2020), but no information is available on sperm chemotaxis in *E. chloroticus*. Future work in this species might combine the impacts of OA on sperm performance, pH_i of both eggs and sperm, and

the chemotactic behaviour of sperm to eggs in OA seawater to increase understanding of sperm-egg interactions in a future ocean.

pH_i

Under control conditions, the pH_i of activated *E. chloroticus* sperm measured with SNARF-1 was 7.52. This pH_i value is consistent with the alkalinisation found in other sea urchins using a range of experimental techniques. Fluorescent amine probes, for example, showed a pH_i increase at activation from pH 6.9-7.0 to ~pH_i 7.4 in buffered artificial seawater (Christen et al., 1982; Lee et al., 1983). Nuclear magnetic resonance (NMR) gave a slightly broader alkalinisation range, from about pH_i 7.0 to 7.4-7.6 in artificial seawaters (Christen et al., 1983; Johnson et al., 1983). SNARF-1 in this study, therefore, provided high-resolution pH_i values that could be used to compare between OA treatments. However, cellular $[K^+]_i$ in *E. chloroticus* sperm (466 mM) is approximately 3-4 times higher than that reported in mammals and at least double that previously determined in sea urchins (Lee et al., 1983; Guerrero and Darszon, 1989; Darszon et al., 2004; reviewed in Supplementary Materials and Methods 2, Table S3). Thus, the use of SNARF-1 in future studies of marine invertebrate sperm needs to use a validated value of $[K^+]_i$.

Internal pH is suggested to play a fundamental role in activating and swimming in sea urchin sperm. The involvement of CO_2 and pH_i is well described (e.g., Christen et al., 1982; Johnson et al., 1983) and has led to the suggestion that sea urchin sperm will be unable to compensate for OA changes in seawater carbonate chemistry, with consequences for activation and motility (Havenhand et al., 2008; Kurihara, 2008; Graham et al., 2015). The effect of OA on pH_i of sea urchin gametes has recently been demonstrated in the unfertilised eggs of *Strongylocentrotus droebachiensis* with a stepped change in pH_i shown at 1000 µatm pCO_2, through changes in un-calibrated fluorescence ratio (R) from the pH-sensitive dye BCECF (Bögner et al., 2014). Under similar conditions in this study, a calibrated stepped decrease in the average pH_i of activated *E. chloroticus* sperm at pH 7.7 (846 µatm pCO_2) confirms OA's suggested significant negative impact.

Why might there be a non-linear decrease in pH_i with pH_e? Although we cannot rule out limitations in the measurement of pH_i, the observation of a stepped-change in the pH_i of unfertilized echinoid eggs using the dye BCECF (Bögner et al., 2014) and SNARF-1 (herein) suggests that this may result from yet-to-be described physiological process(s). For example, an OA-induced disruption of H^+ extrusion from the cell may occur through the lower activity of the voltage and sAC dependent Na^+/H^+ exchanger (Lee, 1985; Neill and Vacquier, 2004).

Reduced exchanger activity might lead to an increased reliance on passive diffusion of H^+ across the cellular membrane (Mohri and Yasumasu, 1963; Hamamah and Gatti, 1998; Missner and Pohl, 2009; Boron et al., 2011). The effects of OA on the maintenance of pH_i may also have knock-on impacts on other cellular processes, including possible involvement in the proposed on/off state of the sperm mitochondrion (Schlegel et al., 2015).

The suggested narcosis of sperm in an elevated pCO_2 world, through the pH_i inhibition of dynein-ATPase activity and bioenergetic pathways, is not supported in this study on *E. chloroticus* sperm. Although the pH sensitivity of dynein-ATPase has been clearly described (Gibbons and Fronk, 1972; Christen et al., 1986; Neill and Vacquier, 2004), this does not appear to be the primary point of regulation under the tested OA treatments, where there was a non-linear decrease in pH_i with experimental changes in pH_e. A similar stepped pattern is seen in other pH-dependent processes, such as the kinetics of the regulatory enzyme sAC, which is also involved in the initiation and maintenance of sperm motility (Nomura et al., 2005; Vacquier et al., 2014). Future research should also investigate the role of pH_i in *E. chloroticus* sperm swimming by using OA treatments that approach the pH_i of sperm within the gonads (pH <7.0). Alternatively, oxygen tension may play a more significant role in sperm activation than currently acknowledged in many OA studies (Cohn, 1918; Mohri and Yasumasu, 1963; Webster and Giese, 1975; Chia and Bickell, 1983; Byrne, 2011), or there may be a role of decreased mitochondrial membrane potential in lower swimming speed (Schlegel et al., 2015).

The relationship between OA, pH_i, sperm activation, and swimming performance in *E. chloroticus* does not appear to be straightforward, with variable OA responses between males, as previously seen in other sea urchins (Schlegel et al., 2012, 2015; Smith et al., 2019). At the same pH_i, sperm from some males showed narcosis that led to a lower proportion of motile sperm (Fig. 5), while others were able to activate sperm with an increased swimming speed (VCL, Fig. 2).

There are two points to note about variability in *E. chloroticus* sperm performance in response to OA. First, all males used in this study were collected from a single location so these results reflect intra-population variability. Adult sea urchins collected from this shallow kelp habitat are exposed to daily pH variability (7.920-8.109; C. Blain unpub. data, see details in Methods) but would be unlikely to experience the pH levels used in our OA treatments (7.77, 7.51). *E. chloroticus* from this location may show potential for genetic adaptation to climate change (temperature, OA), as previously shown in a genotype-by-

environment interaction to increased seawater temperatures during early development (cleavage, gastrulation; Delorme and Sewell, 2016).

Second, *E. chloroticus* is found from the Three Kings Islands (34°10′S) to the Snares Islands (47°60′S), and throughout mainland New Zealand (Barker, 2013). Kapsenberg et al. (2017) have shown that *Strongylocentrotus purpuratus* collected at sites in Oregon and California with different levels of pH variability due to upwelling show differing sensitivities of fertilization to experimental pH. Sea urchins from sites with frequent exposure to low pH required much lower pH treatments to significantly alter fertilization rates and with greater sensitivity in sperm than eggs (Kapsenberg et al., 2017). Similar broad-scale study in *E. chloroticus* across sites with different local pH may test the potential for local adaptation in response to OA.

Conclusion

The hypothesis that sea urchin sperm may exhibit a form of narcosis due to the elevated pCO_2 and low pH of the surrounding seawater was first proposed by Kurihara (2008). Paired analyses of sperm pH_i and sperm motility in *E. chloroticus* showed that sperm could not defend pH_i in future OA conditions and that sperm performance was not a linear pH_i dependent narcosis at low pH_e. Differences in sperm performance, when activated in OA conditions, may also impact fertilization success in *E. chloroticus* in a future ocean.

Acknowledgments:

Thank you for assistance with microscopy (A. Turner), probes (T. Brittian), flow cytometry (A. Brookes), CASA (J. Havenhand), coding and image analysis (R. Gallego, E. Frost), and in the laboratory (M. Clark, D. Baker, I. Ruza, L. van Oosterom). C. Blain generously provided pH data from the collection location. Many thanks to the Reviewers and Editor, whose comments improved the manuscript.

Competing Interests: none

Funding: This work was supported by a Royal Society of New Zealand Marsden Grant to MAS.

References

Adams, N.L., Heyland, A., Rice, L. L., Foltz, K. R. (2019)**.** Procuring animals and culturing of eggs and embryos. *Methods in Cell Biol* **150**, 3-46.

Anderson, M. J., Gorley, R. N. and Clarke, K. R. (2008). *PERMANOVA+ for PRIMER: Guide to software and statistical methods.* Plymouth, UK: PRIMER-E.

Babcock, D. F. (1983). Examination of the intracellular ionic environment and of ionophore action by null point measurements employing the fluorescein chromophore. *J. Biol. Chem.*, **258**, 6380-6389.

Barker M (2013). *Evechinus chloroticus*. In *Developments in aquaculture and fisheries science* (ed. M.L. John), pp. 355–368. Amsterdam: Elsevier.

Bishop, J. (1998). Fertilization in the sea: are the hazards of broadcast spawning avoided when free-spawned sperm fertilize retained eggs? *Proc. Roy. Soc. London -B.* **265**, 725–731.

Bögner, D. (2016). Life under climate change scenarios: Sea urchins' cellular mechanisms for reproductive success. *J. Mar. Sci. Eng.* **4**, 28.

Bögner, D., Bickmeyer, U. and Köhler, A. (2014). CO_2-induced fertilization impairment in *Strongylocentrotus droebachiensis* collected in the Arctic. *Helgoland Mar. Res.* **68**, 341-356.

Bond, J. and Varley, J. (2005). Use of flow cytometry and SNARF to calibrate and measure intracellular pH in NS0 cells. *Cytom. Part A* **64A**, 43-50.

Boron, W. F., Endeward, V., Gros, G., Musa-Aziz, R. and Pohl, P. (2011). Intrinsic CO_2 permeability of cell membranes and potential biological relevance of CO_2 channels. *Chemphyschem* **12**, 1017-1019.

Boryshpolets, S., Kowalski, R. K., Dietrich, G. J., Dzyuba, B. and Ciereszko, A. (2013). Different computer-assisted sperm analysis (CASA) systems highly influence sperm motility parameters. *Theriogenology* **80**, 758-765.

Byrne, M. (2011). Impact of ocean warming and ocean acidification on marine invertebrate life history stages: Vulnerabilities and potential for persistence in a changing ocean. *Oceanogr. Mar. Biol.* **49**, 1-42.

Caldwell, G. S., Fitzer, S., Gillespie, C. S., Pickavance, G., Turnbull, E. and Bentley, M. G. (2011). Ocean acidification takes sperm back in time. *Invertebr. Reprod. Dev.* **55**, 217-221.

Castellini, C., Dal Bosco, A., Ruggeri, S. and Collodel, G. (2011). What is the best frame rate for evaluation of sperm motility in different species by computer-assisted sperm analysis? *Fertil. Steril.* **96**, 24-27.

Chávez, J. C., Darszon, A., Treviño, C.L. and Nishigaki, T. (2020). Quantitative intracellular pH determinations in single live mammalian spermatozoa using the ratiometric dye SNARF-5F. *Front. Cell Dev. Biol.* **7,** 366.

Chia, F. S. and Bickell, L. R. (1983). Spermatogenesis and sperm function: Echinodermata. In *Reproductive biology of invertebrates* Vol. 2 (ed. K. G. Adiyodi and R. G. Adiyodi), pp. 545-620, Chichester: Wiley Interscience.

Christen, R., Schackmann, R. W., Dahlquist, F. W. and Shapiro, B. M. (1983). 31P-NMR analysis of sea urchin sperm activation: Reversible formation of high energy phosphate compounds by changes in intracellular pH. *Exp. Cell Res.* **149**, 289-294.

Christen, R., Schackmann, R. W. and Shapiro, B. M. (1982). Elevation of the intracellular pH activates respiration and motility of sperm of the sea urchin, *Strongylocentrotus purpuratus*. *J. Biol. Chem.* **257**, 14881-14890.

Christen, R., Schackmann, R. W. and Shapiro, B. M. (1986). Ionic regulation of sea-urchin sperm motility, metabolism and fertilizing-capacity. *J. Physiol.- London* **379**, 347-365.

Cohn, E. J. (1918). Studies in the physiology of spermatozoa. *Biol. Bull.* **34**, 167-218.

Crimaldi, J.P., Zimmer, R.K. (2014). The physics of broadcast spawning in benthic invertebrates. *Annu. Rev. Mar. Sci.* **6**, 141-165.

Darszon, A., Wood, C. D., Beltrán, C., Sánchez, D., Rodríguez, E., Gorelik, J., Korchev, Y. E., and Nishigaki, T. (2004). Measuring ion fluxes in sperm. *Methods **Cell*** Biol. **74,** 545-576.

Deaker, D.J., Foo, S.A., Byrne, M. (2019). Variability in egg and jelly-coat size and their contribution to target size for spermatozoa: a review for the Echinodermata. *Mar. Freshwater Res.* **70**, 995–1006

Delorme, N.J., Sewell, M.A. (2016). Genotype‐by‐environment interactions during early development of the sea urchin *Evechinus chloroticus*. *Mar. Biol.* **163,** 215.

Dickson, A. G. (1990). Thermodynamics of the dissociation of boric acid in synthetic seawater from 273.15 to 318.15 K. *Deep-Sea Res.* **37**, 755-766.

Dickson, A. G., Sabine, C. L. and Christian, J. R. (Eds.). (2007). *Guide to best practices for ocean CO_2 measurements*.: PICES Special Publication 3.

Elgeti, J., Kaupp, U. B. and Gompper, G. (2010). Hydrodynamics of sperm cells near surfaces. *Biophys. J.* **99**, 1018-1026.

Fangue, N. A., O'Donnell, M. J., Sewell, M. A., Matson, P. G., MacPherson, A. C. and Hofmann, G. E. (2010). A laboratory-based, experimental system for the study of ocean acidification effects on marine invertebrate larvae. *Limnol. Oceanogr. – Meth.* **8**, 441-452.

Fitzpatrick, J. L., Simmons, L. W. and Evans, J. P. (2012). Complex patterns of multivariate selection on the ejaculate of a broadcast spawning marine invertebrate. *Evolution* **66**, 2451-2460.

Foo, S. A., Deaker, D. and Byrne, M. (2018a)**.** Cherchez la femme – impact of ocean acidification on the egg jelly coat and attractants for sperm. *J. Exp. Biol.* **221**, jeb177188.

Foo, S. A., Byrne, M. and Gambi, M. C. (2018b). Residing at low pH matters, resilience of the egg jelly coat of sea urchins living at a CO_2 vent site. *Mar. Biol.* **165**, 97

García-Soto, J., González-Martínez, M., de De la Torre, L. and Darszon, A. (1987). Internal pH can regulate Ca^{2+} uptake and the acrosome reaction in sea urchin sperm. *Develop. Biol.* **120**, 112-120.

Gee, C. C. and Zimmer-Faust, R. K. (1997). The effects of walls, paternity and ageing on sperm motility. *J. Exp. Biol.* **200**, 3185-3192.

Gibbons, I. R. and Fronk, E. (1972). Some properties of bound and soluble dynein from sea urchin sperm flagella. *J. Cell Biol.* **54**, 365-381.

Graham, H., Rastrick, S. P. S., Findlay, H. S., Bentley, M. G., Widdicombe, S., Clare, A. S. and Caldwell, G. S. (2015). Sperm motility and fertilisation success in an acidified and hypoxic environment. *ICES J. Mar. Sci.*, fsv171.

Guerrero, A. and Darszon, A. (1989). Evidence for the activation of two different Ca2+ channels during the egg jelly-induced acrosome reaction of sea urchin sperm. *J. Biol. Chem.* **264**, 19593-19599.

Guscelli, E., Spicer, J.I., Calosi, P. (2019) The importance of inter-individual variation in predicting species' responses to global change drivers. *Ecol Evol.* https:// doi. org/ 10. 1002/ ece3. 481

Hamamah, S. and Gatti, J.-L. (1998). Role of the ionic environment and internal pH on sperm activity. *Hum. Reprod.* **13 (Suppl 4)**, 20-30.

Hamidinia, S. A., Tan, B., Erdahl, W. L., Chapman, C. J., Taylor, R. W., and Pfeiffer, D. R. (2004). The ionophore nigericin transports Pb^{2+} with high activity and selectivity: A comparison to monensin and ionomycin. *Biochemistry* **43**, 15956-15965.

Havenhand, J. N., Buttler, F. R., Thorndyke, M. C. and Williamson, J. E. (2008). Near-future levels of ocean acidification reduce fertilization success in a sea urchin. *Curr. Biol.* **18**, R651-652.

Ho, M. A., Price, C., King, C. K., Virtue, P. and Byrne, M. (2013). Effects of ocean warming and acidification on fertilization in the Antarctic echinoid *Sterechinus neumayeri* across a range of sperm concentrations. *Mar. Environ. Res*. **90**, 136-141.

Hudson, M. E., Turner, A. and Sewell, M. A. (2015). Comparative ultrastructure of spermatozoa from two regular and two irregular New Zealand echinoids. *Invert. Biol.* **134**, 341-351.

Hurd, C. L., Beardall, J., Comeau, S., Cornwall, C. E., Havenhand, J. N., Munday, P. L., Parker, L. M., Raven, J.A. and McGraw, C. M. (2020). Ocean acidification as a multiple driver: how interactions between changing seawater carbonate parameters affect marine life. *Mar. Freshwater Res.* **71**, 263–274.

IPCC (2014) Climate Change 2014: synthesis report. Contribution of Working Groups I, II and III to the Fifth Assessment Report of the Intergovernmental Panel on Climate Change. Pachauri RK, Meyer LA (eds) IPCC, Geneva, Switzerland, p 151

Johnson, C. H., Clapper, D. L., Winkler, M. M., Lee, H. C. and Epel, D. (1983). A volatile inhibitor immobilizes sea urchin sperm in semen by depressing the intracellular pH. *Develop. Biol.* **98**, 493-501.

Kapsenberg, L., Okamoto, D.K., Dutton, J.M., Hofmann, G.E. (2017). Sensitivity of sea urchin fertilization to pH varies across a natural pH mosaic. *Ecology and Evolution* **2017**, 1-14.

Kurihara, H. (2008). Effects of CO_2-driven ocean acidification on the early developmental stages of invertebrates. *Mar. Ecol. Progr. Ser.* **373**, 275-284.

Lee, H. C. (1985). The voltage-sensitive Na^+/H^+ exchange in sea urchin spermatozoa flagellar membrane vesicles studied with an entrapped pH probe. *J. Biol. Chem.* **260**, 10794-10799.

Lee, H. C., Johnson, C. and Epel, D. (1983). Changes in internal pH associated with initiation of motility and acrosome reaction of sea urchin sperm. *Develop. Biol.* **95**, 31-45.

Levitan, D. R., Sewell, M. A. and Chia, F. S. (1991). Kinetics of fertilization in the sea-urchin *Strongylocentrotus franciscanus*: Interaction of gamete dilution, age, and contact time. *Biol. Bull.* **181**, 371-378.

Levitan, D. R., and Irvine, S.D. (2001). Fertilization selection on egg and jelly-coat size in the sand dollar *Dendraster excentricus*. *Evolution* **55**, 2479-2483.

Lewis, C., Olive, P. J. W., Bentley, M. G. and Watson, G. (2002). Does seasonal reproduction occur at the optimal time for fertilization in the polychaetes *Arenicola marina* L. and *Nereis virens* Sars? *Invertebr. Reprod. Develop.* **41**, 61-71.

Lueker, T. J., Dickson, A. G. and Keeling, C. D. (2000). Ocean pCO_2 calculated from dissolved inorganic carbon, alkalinity, and equations for K_1 and K_2: Validation based on laboratory measurements of CO_2 in gas and seawater at equilibrium. *Mar. Chem.* **70**, 105-119.

Luttikhuizen, P. C., Honkoop, P. J. C. and Drent, J. (2011). Intraspecific egg size variation and sperm limitation in the broadcast spawning bivalve *Macoma balthica*. *J. Exp. Mar. Biol. Ecol.* **396**, 156-161.

Melzner, F., Gutowska, M. A., Langenbuch, M., Dupont, S., Lucassen, M., Thorndyke, M. C., Bleich, M. and Pörtner, H. O. (2009). Physiological basis for high CO_2 tolerance in marine ectothermic animals: Pre-adaptation through lifestyle and ontogeny? *Biogeosciences* **6**, 2313-2331.

Millar, R. B. and Anderson, M. J. (2003). The kinetics of monospermic and polyspermic fertilization in free-spawning marine invertebrates. *J. Theor. Biol.* **224**, 79-85.

Miller, R.L. (1985). Sperm chemo-orientation in the Metazoa. In *Biology of Fertilization Vol. 2* (ed. C. Metz, and A. Monroy), pp. 275-337. New York: Academic Press.

Missner, A. and Pohl, P. (2009). 110 years of the Meyer–Overton rule: Predicting membrane permeability of gases and other small compounds. *ChemPhysChem* **10**, 1405-1414.

Mita, M. and Nakamura, M. (2001). Energy metabolism of sea urchin spermatozoa: The endogenous substrate and ultrastructural correlates. In: *Echinoderm Studies Vol. 6* (ed. M. Jangoux and J. M. Lawrence, pp. 85-110. Meppel, The Netherlands: AA Balkema Publishers, CRC Press.

Mohri, H. and Yasumasu, I. (1963). Studies on the respiration of sea-urchin spermatozoa: V. The effect of pCO_2. *J. Exp. Biol.* **40**, 573-586.

Monroy, A. (1986). A centennial debt of developmental biology to the sea urchin. *Biol. Bull.* **171**, 509-519.

Morita, M., Suwa, R., Iguchi, A., Nakamura, M., Shimada, K., Sakai, K., and Suzuki, A. (2010). Ocean acidification reduces sperm flagellar motility in broadcast spawning reef invertebrates. *Zygote* **18**, 103-107.

Munari, M., Devigili, A., dalle Palle, G., Asnicar, D., Pastore, P., Badocco, D., Marin, M.G. (2022). Ocean acidification, but not environmental contaminants, affects fertilization success and sperm motility in the sea urchin *Paracentrotus lividus*. *J. Mar. Sci. Eng.*, **10**, 247.

Nakagawa, S. and Cuthill, I. C. (2007). Effect size, confidence interval and statistical significance: A practical guide for biologists. *Biol. Rev.* **82**, 591-605.

Nakajima, A., Morita, M., Takemura, A., Kamimura, S. and Okuno, M. (2005). Increase in intracellular pH induces phosphorylation of axonemal proteins for activation of flagellar motility in starfish sperm. *J. Exp. Biol.* **208**, 4411-4418.

Negulescu, P. A. and Machen, T. E. (1990). Intracellular ion activities and membrane transport in parietal cells measured with fluorescent dyes. In: *Methods in Enzymology Vol. 192*, (ed. B. F. Sidney Fleischer), pp. 38-81). London: Academic Press.

Neill, A. T. and Vacquier, V. D. (2004). Ligands and receptors mediating signal transduction in sea urchin spermatozoa. *Reproduction* **127**, 141-149.

Nishigaki, T., José, O., González-Cota, A. L., Romero, F., Treviño, C. L. and Darszon, A. (2014). Intracellular pH in sperm physiology. *Biochem.Bioph. Res. Co.* **450**, 1149-1158.

Nomura, M., Beltrán, C., Darszon, A. and Vacquier, V. D. (2005). A soluble adenylyl cyclase from sea urchin spermatozoa. *Gene* **353**, 231-238.

Okamoto, D.K. (2016). Competition among eggs shifts to cooperation along a sperm supply gradient in an external fertilizer. *Am. Nat.* 187, E129–E142.

Orr, J. C., Epitalon, J. M. and Gattuso, J. P. (2015). Comparison of ten packages that compute ocean carbonate chemistry. *Biogeosciences* **12**, 1483-1510.

Partyka, A., Niżański, W. and Ochota, M. (2012). Methods of assessment of cryopreserved semen. In: *Current Frontiers in Cryobiology*, (ed. P. I. Katkov), pp. 547-574. Rijeka, Croatia: InTech.

Perez, F. F. and Fraga, F. (1987). Association constant of fluoride and hydrogen ions in seawater. *Mar. Chem.* **21**, 161-168.

Pistevos, J.C.A., Calosi, P., Widdicombe, S., Bishop, J.D.D. (2011) Will variation among genetic individuals influence species responses to global climate change? *Oikos* **120**, 675-689.

Podolsky, R.D. (2002). Fertilization ecology of egg coats: physical versus chemical contributions to fertilization success of free-spawned eggs. *J. Exp. Biol.* **205**, 1657-1668.

Pressman, B. C. (1976). Biological applications of ionophores. *Ann. Rev. Biochem.* **45**, 501-530.

Purchase, C. F. and Earle, P. T. (2012). Modifications to the IMAGEJ computer assisted sperm analysis plugin greatly improve efficiency and fundamentally alter the scope of attainable data. *J. Appl. Ichthyol.* **28**, 1013-1016.

Quinn, G. P. and Keough, M. J. (2002). *Experimental design and data analysis for biologists*. Cambridge, UK: Cambridge University Press.

Ramírez-Gómez, H.V., Sabinina, V.J., Pérez, M.V., Beltran, C., Carneiro, J., Wood, C.D., Tuval, I., Darszon, A., Guerrero, A. (2020). Sperm chemotaxis is driven by the slope of the chemoattractant concentration field. *eLife* **9**, e50532.

RCoreTeam (2015). *R: A language and environment for statistical computing* (Version 3.1.3). R Foundation for Statistical Computing, Vienna, Austria. Retrieved from http://www.R-project.org/

Reuter, K. E., Lotterhos, K. E., Crim, R. N., Thompson, C. A. and Harley, C. D. G. (2011). Elevated pCO_2 increases sperm limitation and risk of polyspermy in the red sea urchin *Strongylocentrotus franciscanus*. *Global Change Biol*. **17**, 2512-2512.

Riddell, F. G., Arumugam, S., Brophy, P. J., Cox, B. G., Payne, M. C. H. and Southon, T. E. (1988). The nigericin-mediated transport of sodium and potassium ions through phospholipid bilayers studied by sodium-23 and potassium-39 NMR spectroscopy. *J. American Chem. Soc.* **110**, 734-738.

Riebesell, U., Fabry, V. J., Hansson, L. and Gattuso, J.-P. (Eds.). (2010). *Guide to best practices for ocean acidification research and data reporting*. Luxembourg: Publications Office of the European Union.

Schlegel, P., Binet, M. T., Havenhand, J. N., Doyle, C. J. and Williamson, J. E. (2015). Ocean acidification impacts on sperm mitochondrial membrane potential bring sperm swimming behaviour near its tipping point. *J. Exp. Biol.* **218**, 1084-1090.

Schlegel, P., Havenhand, J. N., Gillings, M. R. and Williamson, J. E. (2012). Individual variability in reproductive success determines winners and losers under ocean acidification: A case study with sea urchins. *PLoS ONE* **7**, e53118.

Sewell, M. A., Millar, R. B., Yu, P. C., Kapsenberg, L. and Hofmann, G. E. (2014). Ocean acidification and fertilization in the Antarctic sea urchin *Sterechinus neumayeri*: The importance of polyspermy. *Envir. Sci. Tech.* **48**, 713-722.

Sewell, M. A., Baker, D.W., Hudson, M.E., Millar, R. B. and Hickey, A. J. R. (2021). Near-future oceanic CO_2 delays development and growth in early-stage larvae of the endemic New Zealand sea urchin, *Evechinus chloroticus*. *Mar. Biol.* 168, 141

Smith, K.E., Byrne, M., Deaker, D., Hird, C.M., Nielson, C., Wilson-McNeal, A. and Lewis, C. (2019). Sea urchin reproductive performance in a changing ocean: poor males improve while good males worsen in response to ocean acidification. *Proc. R. Soc. B* **286**, 20190785.

Thomas, J. A., Buchsbaum, R. N., Zimniak, A. and Racker, E. (1979). Intracellular pH measurements in Ehrlich ascites tumor cells utilizing spectroscopic probes generated in situ. *Biochemistry* **18**, 2210-2218.

Tosti, E. (1994). Sperm activation in species with external fertilisation. *Zygote* **2**, 359–361.

Trimmer, J. S. and Vacquier, V. D. (1986). Activation of sea-urchin gametes. *Annu. Rev. Cell Biol.* **2**, 1-26.

Uppström L. R. (1974). The boron/chlorinity ratio of deep-sea water from the Pacific Ocean. *Deep Sea Res.Oceanogr. Abstracts* **21**, 161-162.

Vacquier, V. D., Loza-Huerta, A., García-Rincón, J., Darszon, A. and Beltrán, C. (2014). Soluble adenylyl cyclase of sea urchin spermatozoa. *BBA – Mol. Basis Dis.* **1842**, 2621-2628.

Vogel, H., Czihak, G., Chang, P. and Wolf, W. (1982). Fertilization kinetics of sea-urchin eggs. *Math. Biosci.* **58**, 189-216.

Webster, S. K. and Giese, A. C. (1975). Oxygen consumption of the purple sea urchin with special reference to the reproductive cycle. *Biol. Bull.* **148**, 165-180.

Wieder, E. D., Hang, H., and Fox, M. H. (1993). Measurement of intracellular pH using flow cytometry with carboxy-SNARF-1. *Cytometry*, **14**, 916-921.

Wilson-Leedy, J. G. and Ingermann, R. L. (2007). Development of a novel CASA system based on open source software for characterization of zebrafish sperm motility parameters. *Theriogenology* **67**, 661-672.

Wood, C., Guerrero, A., Priego-Espinosa, D.A., Martĭnez-Mekler, G., Carneiro, J., Darszon, A. (2015). Sea urchin sperm chemotaxis. In *Flagellar Mechanics and Sperm Guidance* (ed. J. J. Cosson), pp. 135-182. UAE: Bentham Science Publishers.

Figures and Tables

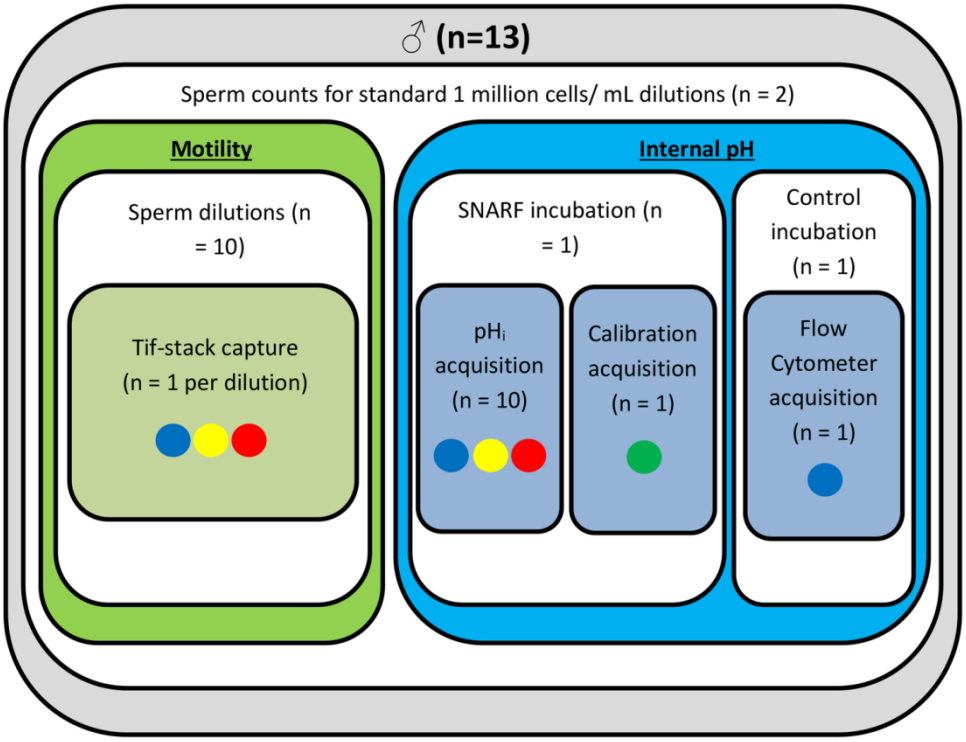

Fig. 1. Infographic of sperm motility and internal pH experiments for each male (n = 13). Coloured circles represent OA seawaters (blue = Control; yellow = RCP 8.5 at 2100; red = RCP 8.5 at 2150), and calibration series (green). Levels of replication for each measurement are shown in brackets.

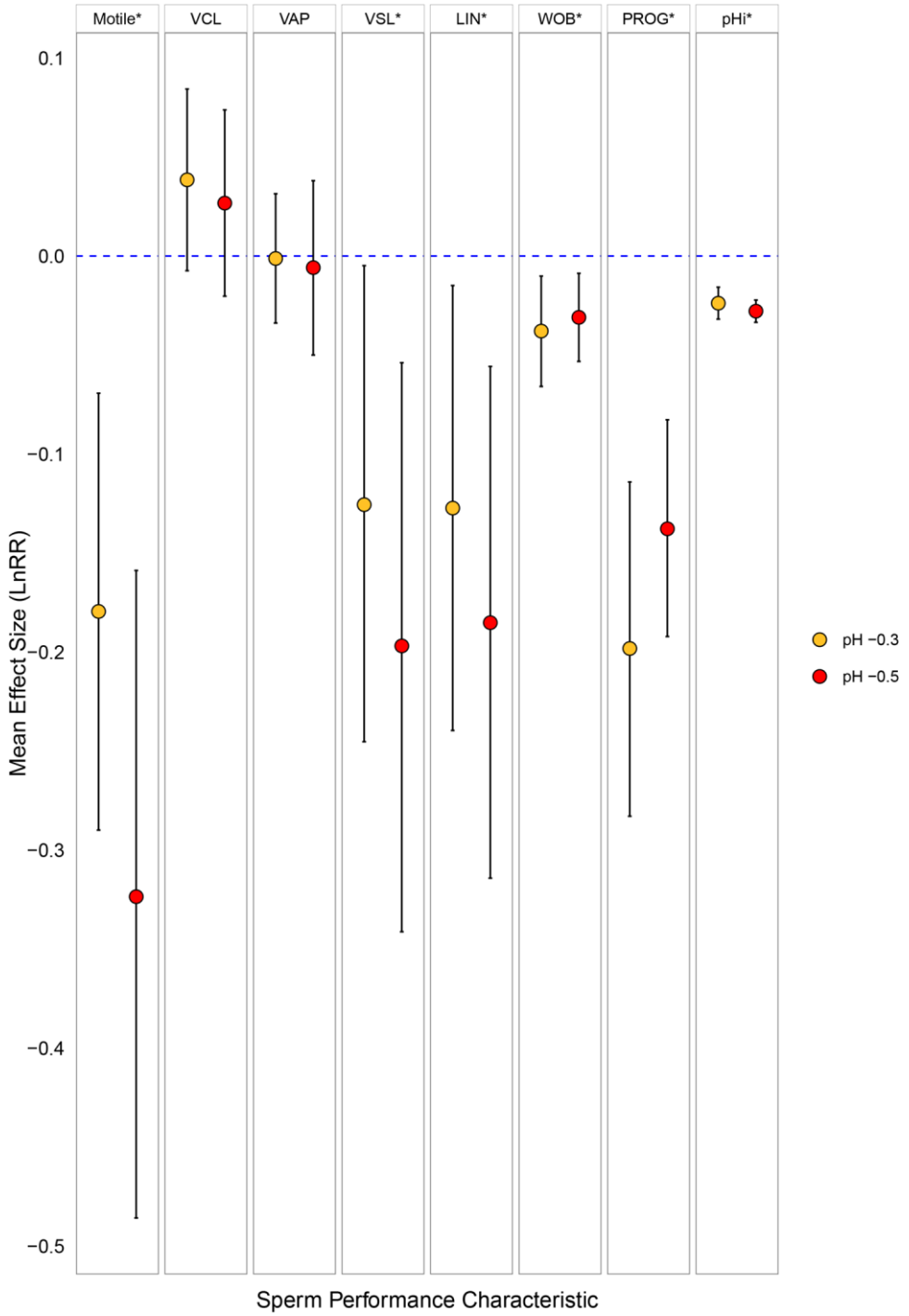

Fig. 2. Average effect size of elevated pCO_2 seawaters on sperm performance characteristics using natural-log response ratio (LnRR). Bootstrap means (100,000 times) with 95% confidence intervals (error bars); blue dashed line represents zero effect of pCO_2 seawater. Yellow data points are effect size of RCP 8.5 at 2100 (or -0.32 pH units from Control); red are RCP 8.5 at 2150 (-0.58 pH units from Control). Motile = proportion motile; VCL = velocity curvilinear ($\mu m.s^{-1}$); VAP = velocity average path ($\mu m.s^{-1}$); VSL = velocity straight line ($\mu m.s^{-1}$); LIN

= linearity; PROG = progression; pH_i = internal pH (n = 13 with technical replication of 9 or 10 for each male at each OA treatment level). Significant differences are where 95% confidence interavals do not overlap with zero and are indicated by an * in the Label row.

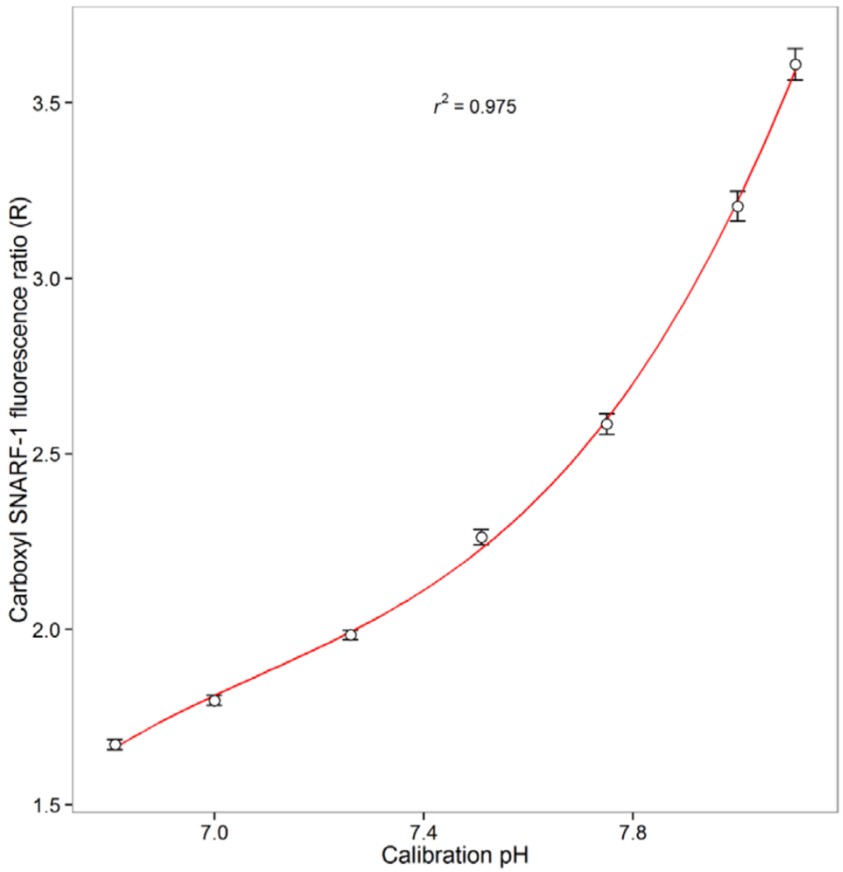

Fig. 3. Calibration curve for internal pH of sperm cells using SNARF-1 and nigericin (n = 14, error bars = s.e.m.). Fluorescence ratio (R) calculated from FL3/FL2. Red line = linear regression 3rd order polynomial.

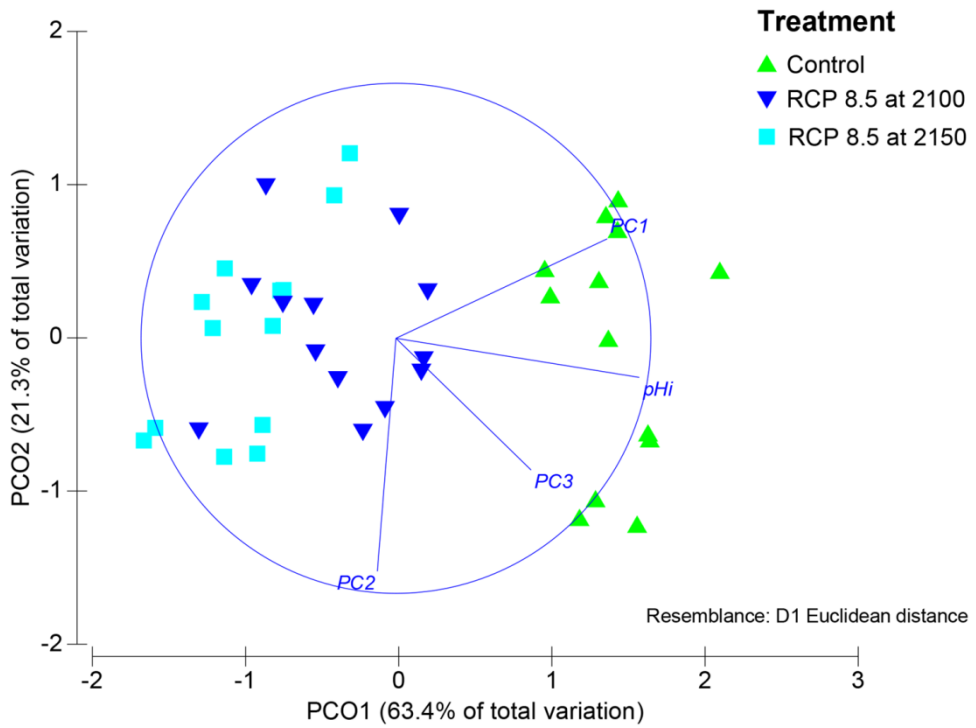

Fig. 4. Principal coordinate ordination (PCO) of sperm performance parameters in elevated pCO_2 seawaters. Control, RCP 8.5 at 2100, RCP 8.5 at 2150 (N= 13 males). Eigenvalues for vector overlay are in Table 4.

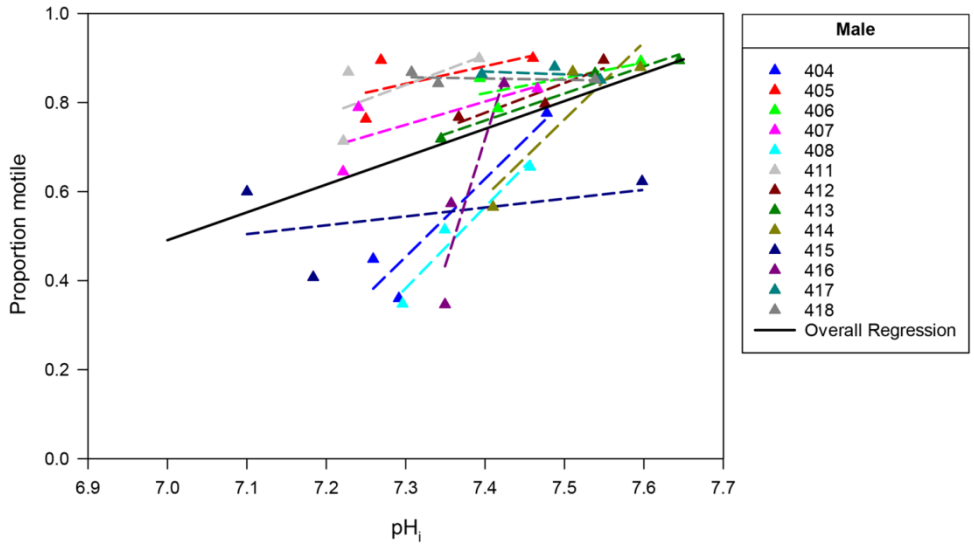

Fig. 5. Relationship between internal pH (pH_i) and % motility of *E. chloroticus* sperm cells in elevated pCO_2 seawaters: Control, RCP 8.5 at 2100, RCP 8.5 at 2150 for the 13 males. Symbols and dashed regression line are colour-coded for each male. Solid regression line = average response. Proportion motile = -3.884 + (0.625 * pH_i); N= 39; r^2 = 0.224.

Table 1. Measures of sperm motility and performance parameters extracted from ImageJ CASA macro output.

Parameter	***Description***	***Units***
Sperm motility	Proportion of sperm moving in a manner fitting motility determination parameters	-
Velocity curvilinear (VCL)	Average velocity over entire track (total distance travelled) per second	$\mu m.s^{-1}$
Velocity average path (VAP)	Average path velocity based on a roaming average of 5 2/3 frames (1/6th of the frame rate).	$\mu m.s^{-1}$
Velocity straight line (VSL)	Straight line velocity between the first and last points of the average path	$\mu m.s^{-1}$
Linearity (LIN)	Linearity given by VSL/VAP, describing path curvature	-
Wobble (WOB)	VAP/VCL, describes side to side movement of the sperm head	-
Progression (PROG)	The average distance of the sperm from its origin on the average path during all frames analysed	µm

Table 2. OA Treatment seawater parameters: Control, RCP 8.5 at 2100, and RCP 8.5 at 2150. Measured values of pH_{Total} (mean ± s.e.m.) and total alkalinity (TA) used with salinity and experimental temperature (T, constant in the temperature block) to calculate (using seacarb R-package) the carbonate parameters of pCO_2 and saturation states for calcite (Ω_{Ca}) and aragonite (Ω_{Ar}). All experiments were conducted with four batches of seawater (N= 4).

OA treatment	pH_{Total}	T (˚C)	Salinity	TA (µequiv kg^{-1})	pCO_2 (µatm)	Ω_{Ca}	Ω_{Ar}
Control	8.09 ± 0.01	20	34.4 ± 0.0	2308 ± 7.66	354.4 ± 7.63	4.79 ± 0.059	3.11 ± 0.038
RCP 8.5 at 2100	7.77 ± 0.03	20	34.5 ± 0.0	2314 ± 5.62	846.4 ± 33.22	2.57 ± 0.075	1.67 ± 0.048
RCP 8.5 at 2150	7.51 ± 0.02	20	34.4 ± 0.0	2309 ± 10.43	1623.7 ± 41.77	1.48 ± 0.030	0.95 ± 0.020

Table 3. Sperm performance characteristics (mean ± s.e.m.) in different OA treated seawaters (N = 13 males, with technical replication of 9 or 10 for each male at each OA treatment level).

	OA Treatment		
	Control	**RCP 8.5 at 2100**	**RCP 8.5 at 2150**
Sperm Performance	***pH 8.09***	***pH 7.77***	***pH 7.51***
Motility = proportion of motile sperm	0.83 ± 0.03	0.74 ± 0.04	0.64 ± 0.06
VCL = velocity curvilinear (µm.s^{-1})	125.61 ± 3.48	128.78 ± 1.63	128.43± 1.38
VAP = velocity average path (µm.s^{-1})	100.87 ± 1.78	100.33 ± 0.97	99.19 ± 1.79
VSL = velocity straight line (µm.s^{-1})	162.76 ± 8.80	141.60 ± 6.79	133.64 ± 9.64
LIN = linearity	1.61 ± 0.08	1.41 ± 0.06	1.35 ± 0.09
WOB = head wobble	0.81 ± 0.01	0.78 ± 0.01	0.77 ± 0.01
PROG = progression	317.45 ± 16.83	262.25 ± 11.35	271.35 ± 15.27
pH_i	7.52 ± 0.02	7.35 ± 0.04	7.31± 0.02

Table 4. Eigenvalues from principal component analysis of standardised ($\overline{x}$, σ) sperm motility and CASA (computer assisted sperm analysis) output variables from *E. chloroticus* sperm (N = 13 males, with technical replication of 9 or 10 for each male at each OA treatment level).

Variable	PC1	PC2	PC3	pH_i
Motility = proportion	0.284	-0.05	0.276	-0.626
VCL = velocity curvilinear ($\mu m.s^{-1}$)	0.001	-0.62	-0.540	-0.057
VAP = velocity average path ($\mu m.s^{-1}$)	0.325	-0.625	0.068	0.299
VSL = velocity straight line ($\mu m.s^{-1}$)	0.561	0.220	-0.329	0.137
LIN = linearity	0.504	0.367	-0.357	0.072
WOB = head wobble	0.391	-0.101	0.622	0.377
PROG = progression	0.304	-0.171	0.071	-0.591
Eigenvalue	2.36	1.58	1.15	0.958
% Variation Explained	34.9	23.3	17.0	14.1
Cumulative % Variation	34.9	58.2	75.2	89.3

A

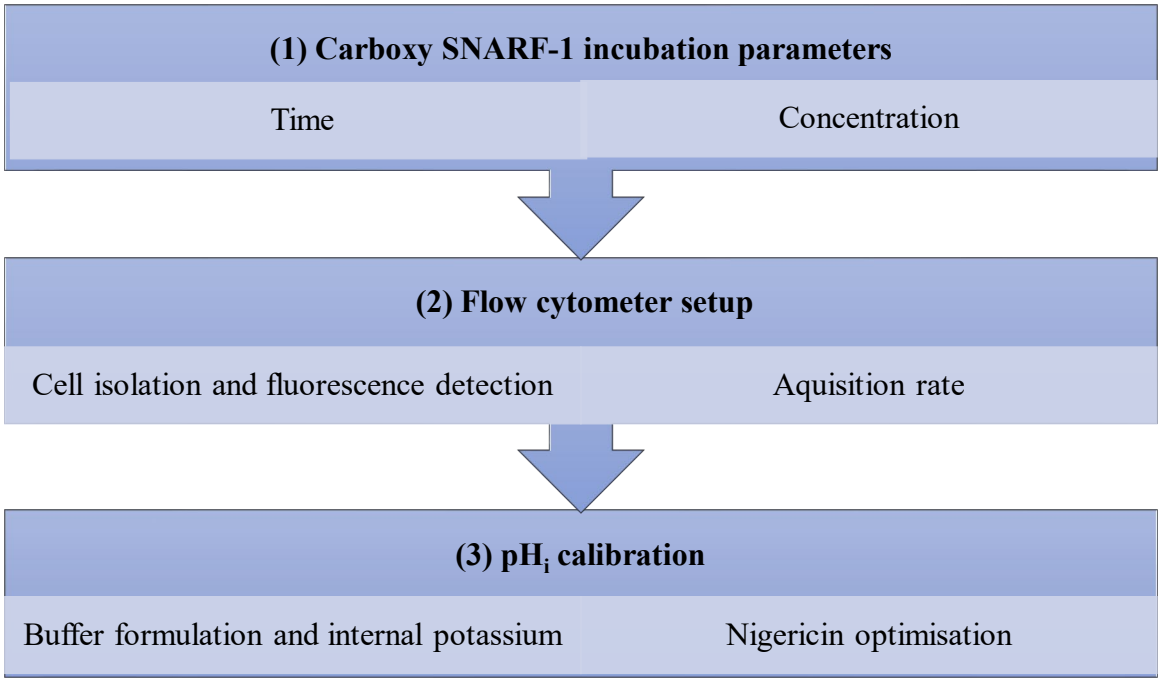

B

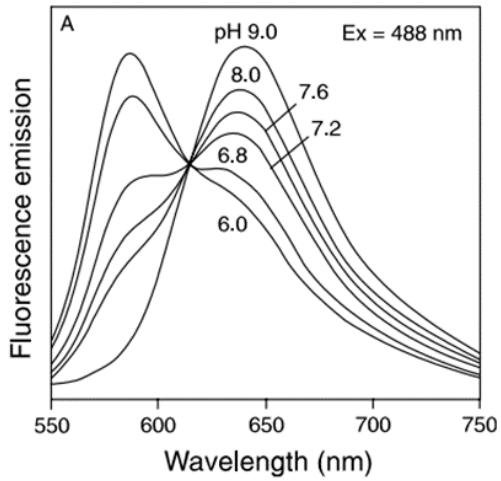

C

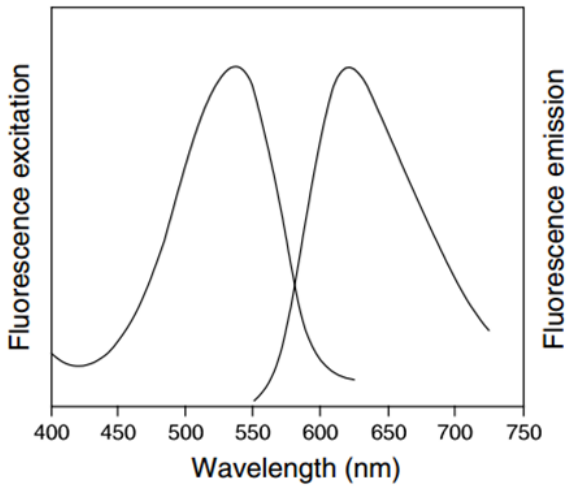

Fig. S1. A. Key steps in development of SNARF-1 incubation and analysis protocol: (1) Incubation time and concentration for optimised fluorescence signal; (2) flow cytometer parameterisation for excitation of SNARF-1 and emission acquisition; and (3) pHi calibration accuracy dependent on correct buffer formulation and nigericin incubation conditions. B. Emission spectra of SNARF-1 in 50 mM potassium phosphate buffers at various pH values with samples excited at 488 nm. C. Fluorescence excitation and emission profile of propidium iodide bound to double-stranded DNA. B) and C) modified from Molecular Probes (2010).

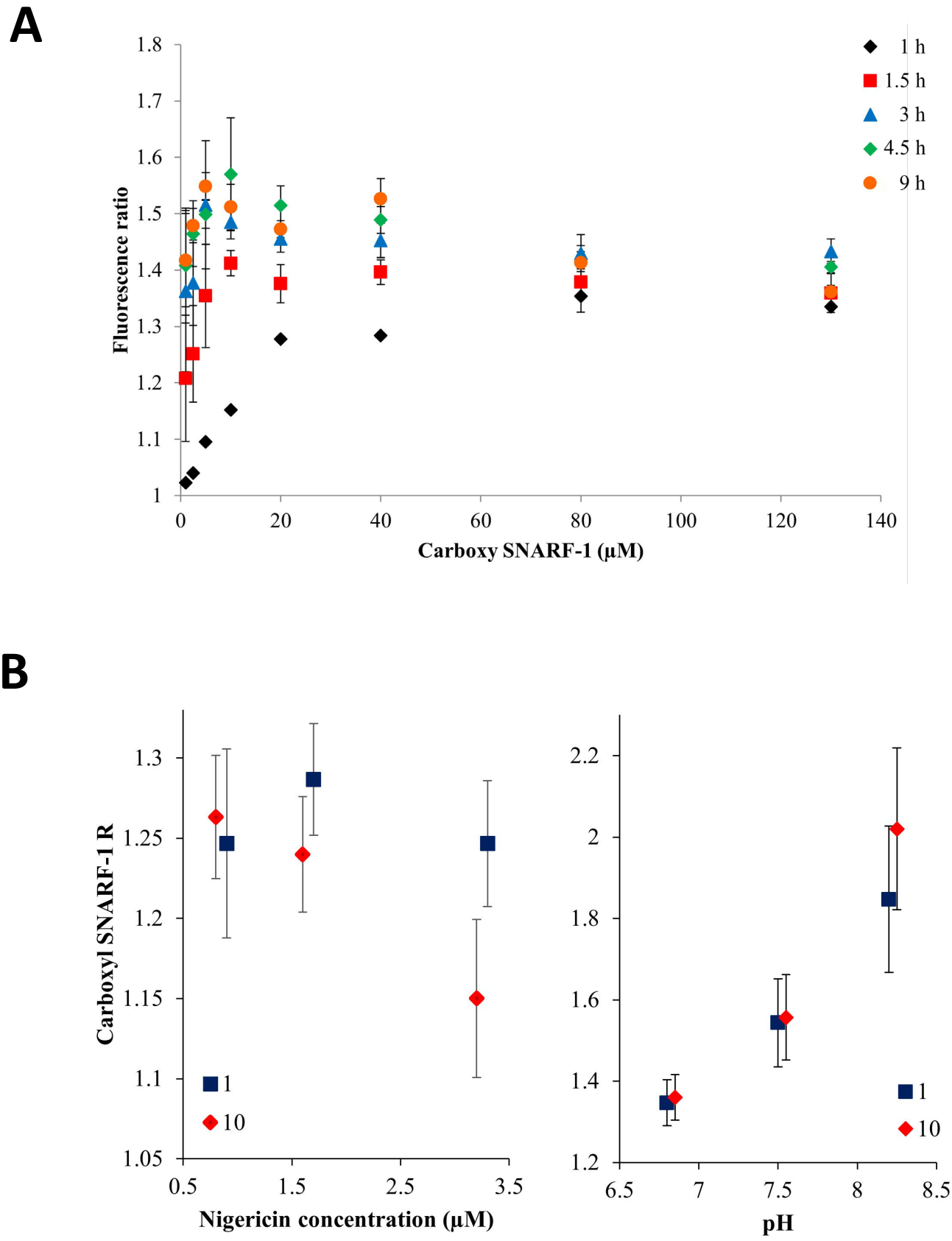

Fig. S2. A. SNARF-1 fluorescence ratio for different incubation conditions (time and concentration) n = 3. Time of incubation is given in the legend. **B.** Nigericin-induced shift in carboxyl SNARF-1 fluorescence ratio (R) from *E. chloroticus* sperm cells after 1 (blue square) and 10 minute (red diamond) nigericin incubations. Left panel shows results for different nigericin concentrations. Right panel shows results for different buffer pH at 1µM nigericin. Data points are offset for clarity (n = 3).

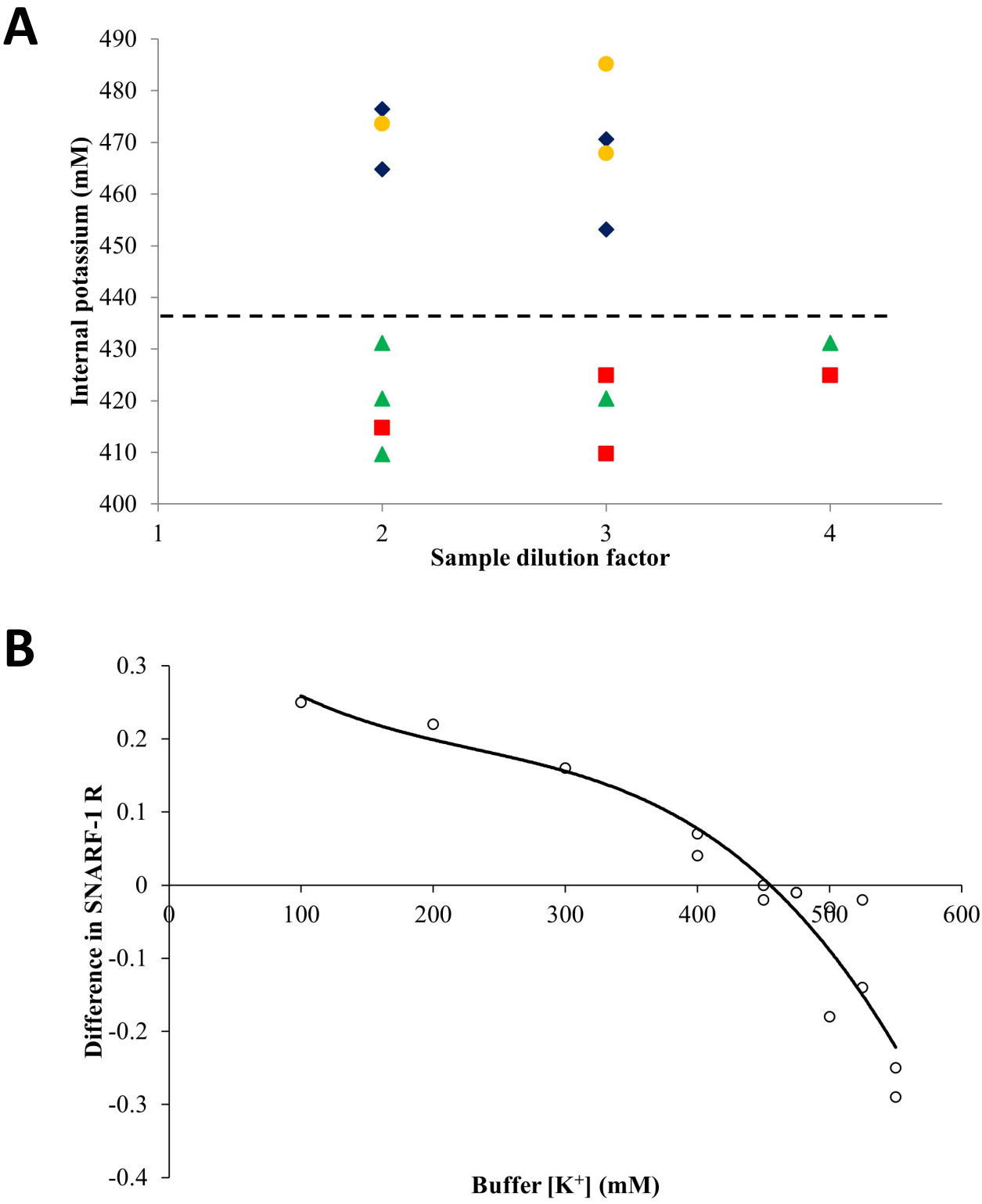

Fig. S3. A. $[K^+]_i$ across different sample dilutions from the blood gas analyser (n = 6, with technical replication at each sample dilution from 1 to 3); different individuals in different colours; dashed line = average of individuals [436 mM]). **B.** SNARF-1 emission ratios (R) across a $[K^+]$ gradient at buffer pH 7.5 in sperm cells of *Evechinus chloroticus*. Differences calculated from R of fresh sperm. Internal $[K^+]$ equalised with buffer $[K^+]$ using nigericin (n = 2), relationship described with a third order polynomial regression line.

Table S1. Parameterisation for sperm motility analysis. Input parameters and their function in the analysis of Evechinus chloroticus sperm, using CASA package for ImageJ.

	Input code	Input description	Value	Notes
Defining sperm heads	a	Minimum sperm size (pixels)	5	Set to ensure background noise was not identified as sperm cells
	b	Maximum sperm size (pixels)	300	Set to ensure that large distorted sperm are captured as a single sperm trail, not divided into separate sperm trails. But to exclude refractive rings
	c	Minimum track length (frames)	10	Set to minimise inclusion of sperm cells swimming vertically through the field of view, but sufficient to capture drifting immotile sperm
	d	Maximum sperm velocity between frames (pixels)	20	Optimised for realistic, smooth sperm tracks
Defining motility	e	Minimum VSL for motile (µm/s)	6	Below this value sperm are categorised as immotile. This is set to allow for bulk fluid flow and immotile sperm drift
	f	Minimum VAP for motile (µm/s)	8	Set to ensure non-directional swimming sperm are included in % motility calculations
	g	Minimum VCL for motile (µm/s)	15	
Speed filter 1	h	Low VAP speed (µm/s)	10	Less than this value (but above "f") defines "low" VAP
	i	Maximum % of path with zero VAP	1	Sperm classed as motile if greater than 1% of sperm track is above "f"
	j	Maximum % of path with low VAP	50	Sperm classed as motile if greater than 50% of sperm track is above "h"
Filter 2	k	Low VAP speed 2 (µm/s)	30	Above this set of conditions identifies sperm moving faster than is characteristic of bulk flow regardless of their motion characteristics (Wilson-Leedy and Ingermann, 2007).
	l	Low VCL speed (µm/s)	35	
Filter 3	m	High WOB (% VAP/VCL)	80	This set of conditions is intended to find sperm that are in motion for most of the time analysed and that do not move in a perfectly straight line; as would be expected of sperm moving due to bulk flow (Wilson-Leedy and Ingermann, 2007).
	n	High LIN (% VSL/VAP)	80	

Filter 4	o	High WOB two (% VAP/VCL)	80	This set of conditions identifies slow moving sperm with a high degree of path curvature, as such curvature is not characteristic of sperm moving due to bulk flow (Wilson-Leedy and Ingermann, 2007)
	p	High LIN two (% VSL/VAP)	80	
	q	Frame rate (frames per sec)	34	Frame rate of video acquisition
	r	Microns per 1000 pixels	730	Calibrated in ImageJ using a micrometer to give an average 137.018 (SE = 0.23; n = 10) pixels per 0.1 mm
	s	Print xy co-ordinates for all tracked sperm?	0	Not used
	t	Print motion characteristics for all sperm?	0	Not used
	u	Print median values for motion characteristics?	0	Not used

Table S2. Summary of internal potassium concentration [K⁺ 1, ICP-OES = inductively coupled plasma – optical absorpt]iio nof s Ep.e ccthrloosrcootipcyu;s M speethrmod f o2r, BMleotohdo d gas analysis, and Method 3, SNARF-1 null-point measurements using nigericin. Replication indicated in brackets, with null-point [K⁺]i value from linear regression calculation.

Method	**$[K^+]_i$ (mM)**
1: ICP-OES	498 ± 34 (n = 3)
2: Blood gas analysis	436 ± 33 (n = 6)
3: Null-point measurements	463.6 (n = 2)

Table S3. A. Experimentally derived values of $[K^+]_i$ for a range of organisms and a variety of tissue and cell types. Concentrations are listed in descending order for different taxa. The analytical techniques and nigericin values are included where stated (- = not applicable). B. Source of [K+]i values used for a range of tissues and cells in new study organisms. Where possible, source identifies original study organism and citation. Concentrations listed in descending order for different taxa.

A. Experimentally derived values of $[K^+]_i$

$[K^+]_i$ mM	Organism	Nigericin (µg/ml)	Analytical technique	Reference
480	Cnidarian tentacle	-	"intracellular ion contents obtained by subtracting the extracellular ion content from total tissue content"	Herrera et al. (1989)
301	Cnidarian body wall	-		
215	Sea urchin - eggs	-	Micro electrode	Shen and Sui (1989)
210	Sea urchin – sperm	15	Using method from Hallam and Tashjian Jr (1987), (Na^+ was replaced by an equimolar $[K^+]$)	Guerrero and Darszon (1989); Darszon et al. (2004)
120 to 300+	Sea urchin - sperm	-	Nigericin null-point 9AA uptake ratio	Lee et al. (1983)
125 to 175	Sea urchin - sperm (hypotonically swollen)	-	Swollen sperm – BCECF null-point with nigericin	Babcock et al. (1992)
111.5	*Evechinus chloroticus* muscle tissue	-	FAAS	Emily Frost (personal communication)
147.8	*E. chloroticus* gut and nerve tissue	-	FAAS	

105	Puffer Fish – sperm	20	Methodology undetermined	Takai and Morisawa (1995)
120	Bovine - sperm	2 nmol	Fluorescein Null-point with nigericin	Babcock (1983)
120	Hamster - ovary	5	third-order polynomial	Wieder et al. (1993)
137	Human lymphocytes	3	BCECF null-point with nigericin	Balkay et al. (1997)
74	Human - U266	3		
96	Human - JY	3		
106	Human - HUT-78	3		
110	Mammal	20	Not stated	Cody et al. (1993)
146	Mouse - Balb/c-3T3	5	FAAS	Giuliano and Gillies (1987)
139	Mouse lymphocytes	3	BCECF null-point with nigericin	Balkay et al. (1997)
147 to 175	Mice - tumour	-	Determined – flame photometer	Lassen et al. (1971)
130	Rat - pituitary cells	50	Calibration on lysed cells, using extracellular readings	Hallam and Tashjian Jr (1987)
140	Rat – carotid bodies	-	Not stated	Buckler and Vaughan-Jones (1990)
120	Rabbit - gland	10-50	Approximation	Negulescu and Machen (1990)
122.8	Rabbit – kidney tubules	20	Not stated	Dubbin et al. (1993)
110	Rat - skeletal muscle	20	Not stated	Cody et al. (1993)
140	Rat - cardiac myocytes	10	Not stated	Wu et al. (1994)
140	Rat – carotid bodies	10	Not stated	Richmond and Vaughan-Jones (1997)
135	Rat - lymphocytes	3	BCECF null-point with nigericin	Balkay et al. (1997)
60	Common carp sperm	3	BCECF null-point with nigericin	Balkay et al. (1997)
63	Carp – sperm - quiescent	-	Nigericin pH determination (however, false assumption of no alteration of $[K^+]$)	Krasznai et al. (2003)
37	Carp –sperm - 20 s after activation	-		
22	Carp – sperm - 60 s after activation	-		
20	Carp – sperm - 300 s after activation	-		

B. Source of $[K^+]_i$ values.

$[K^+]_i$ mM	New study organism	Original study organism and source	New study reference
200	Coral	From anemone - Herrera et al. (1989)	Venn et al. (2009)
Not stated	Coral	Not explicitly stated but implied from previous study (Venn et al., 2009)	Gibbin et al. (2014)
200 to 240	Sea urchin - eggs	Various studies	Tupper (1973) and Robinson (1976) In Shen and Sui (1989)
210	Sea urchin – sperm	Unclear. Involved replacing Na^+ by an equimolar $[K^+]$	Guerrero and Darszon (1989); Darszon et al. (2004)
180	Sea urchin - sperm	From sea urchin sperm, in Babcock et al. (1992)	Beltran et al. (2014)
150	Sea urchin pluteus	From *Emiliania huxleyi* and urchin egg [hard to determine]	Stumpp et al. (2012)
120-130	Starfish - sperm	From bovine + mice + rabbit in Negulescu and Machen (1990), Babcock (1983) and Thomas et al. (1979)	Nakajima et al. (2005)
140	Glial	From hamsters, in Martinez-Zaguilan et al. (1996)	Sánchez-Armáss et al. (2006)
148	Hamster - Insulin-secreting HIT-T15 cells	From mouse, in Martinez-Zaguilan et al. (1991)	Martinez-Zaguilan et al. (1996)
140	Human – NS0	From mouse, in Thomas et al. (1979)	Bond and Varley (2005)
130	Mouse – tumour	From mouse, in Lassen et al. (1971)	Thomas et al. (1979)
146	Mouse – embryo fibroblasts	From mouse, in Giuliano and Gillies (1987)	Martinez-Zaguilan et al. (1991)
105	Rat - astrocytes	From mouse, in Thomas et al. (1979)	Bevensee et al. (1997)
100-260	*Emiliania huxleyi*	*E. huxleyi* in Sikes & Wilbur (1982); Ho et al. (2003)	Suffrian et al. (2011)